Chordal force profile after neochordal repair of anterior mitral valve prolapse: An ex vivo study

Shin Yajima, MD, PhD,[a] Yuanjia Zhu, MD, MS,[a,b] Charles J. Stark, MS,[a] Robert J. Wilkerson, BS,[a] Matthew H. Park, MS,[a,c] Elde Stefan, MD,[a] and Y. Joseph Woo, MD[a,b]

ABSTRACT

Objective: This study aimed to biomechanically evaluate the force profiles on the anterior primary and secondary chordae after neochord repair for anterior valve prolapse with varied degrees of residual mitral regurgitation using an ex vivo heart simulator.

Methods: The experiment used 8 healthy porcine mitral valves. Chordal forces were measured using fiber Bragg grating sensors on primary and secondary chordae from A2 segments. The anterior valve prolapse model was generated by excising 2 primary chordae at the A2 segment. Neochord repair was performed with 2 pairs of neochords. Varying neochord lengths simulated postrepair residual mitral regurgitation with regurgitant fraction at >30% (moderate), 10% to 30% (mild), and <10% (perfect repair).

Results: Regurgitant fractions of baseline, moderate, mild, and perfect repair were 4.7% ± 0.8%, 35.8% ± 2.1%, 19.8% ± 2.0%, and 6.0% ± 0.7%, respectively ($P < .001$). Moderate had a greater peak force of the anterior primary chordae (0.43 ± 0.06 N) than those of baseline (0.19 ± 0.04 N; $P = .011$), mild (0.23 ± 0.05 N; $P = .041$), and perfect repair (0.21 ± 0.03 N; $P = .006$). In addition, moderate had a greater peak force of the anterior secondary chordae (1.67 ± 0.17 N) than those of baseline (0.64 ± 0.13 N; $P = .003$), mild (0.84 ± 0.24 N; $P = .019$), and perfect repair (0.68 ± 0.14 N; $P = .001$). No significant differences in peak and average forces on both primary and secondary anterior chordae were observed between the baseline and perfect repair as well as the mild and perfect repair.

Conclusions: Moderate residual mitral regurgitation after neochord repair was associated with increased anterior primary and secondary chordae forces in our ex vivo anterior valve prolapse model. This difference in chordal force profile may influence long-term repair durability, providing biomechanical evidence in support of obtaining minimal regurgitation when repairing mitral anterior valve prolapse. (JTCVS Open 2023;15:164-72)

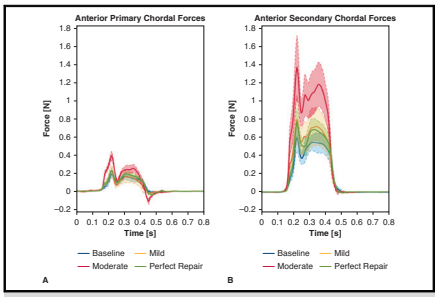

Moderate residual MR had a greater force on native chordae than did mild and perfect repair.

CENTRAL MESSAGE

The peak stress on the anterior primary and secondary chordae is significantly greater in moderate residual MR postrepair than that in mild residual MR.

PERSPECTIVE

Moderate residual MR postneochord repair for anterior valve prolapse was associated with increased anterior primary and secondary chordae forces in our ex vivo model compared with mild residual MR. This difference in chordal force profile may influence long-term repair durability, providing biomechanical evidence supporting obtaining minimal regurgitation when repairing mitral anterior valve prolapse.

Video clip is available online.

Mitral regurgitation (MR) is the most representative phenotype of heart valve disease requiring surgical correction. According to a report from the Society of Thoracic Surgeons Adult Cardiac Surgery Database, approximately

From the Departments of [a]Cardiothoracic Surgery, [b]Bioengineering, and [c]Mechanical Engineering, Stanford University, Stanford, Calif.

Supported by the National Institutes of Health (NIH) (grant Nos. NIH R01 HL152155 to Dr Woo; and NIH F32 HL158151 to Dr Zhu), the Japan Heart Foundation (Dr Yajima), and the Thoracic Surgery Foundation Resident Research Fellowship (Dr Zhu). The content is solely the responsibility of the authors and does not necessarily represent the official views of the funders.

Read at the 103rd Annual Meeting of The American Association for Thoracic Surgery, Los Angeles, California, May 6-9, 2023.

Received for publication Jan 20, 2023; revisions received April 17, 2023; accepted for publication April 17, 2023; available ahead of print June 1, 2023.

Address for reprints: Y. Joseph Woo, MD, Department of Cardiothoracic Surgery, Falk Cardiovascular Research Center, Stanford University School of Medicine, 300 Pasteur Dr, Stanford, CA 94305 (E-mail: joswoo@stanford.edu).

2666-2736

https://doi.org/10.1016/j.xjon.2023.04.011

Abbreviations and Acronyms
3D = 3-dimensional
AVP = anterior mitral valve prolapse
LV = left ventricle
MAP = mean arterial pressure
MR = mitral regurgitation
MV = mitral valve
RF = regurgitant fraction

120,000 patients with MR underwent mitral valve (MV) repair in the United States in 2019, with the volume increasing by 77% compared with the previous decade.[1] Residual postrepair MR has been a great concern and is known to influence mortality and induce adverse left ventricular (LV) remodeling, recurrence of significant MR, and reoperation.[2-15] Residual MR has been reported to be associated with recurrent severe MR resulting in reoperation,[2,4,6,8,10] even in mild cases.[3,5,9,14] In addition, the prevalence of significant MR after MV repair is relatively higher in anterior valve prolapse (AVP) repair compared with posterior valve prolapse repair.[3,5,7,9] Recurrent leaflet prolapse has been reported to be among the most common reasons for recurrent MR after MV repair.[16] However, underlying biomechanical evidence supporting the mechanism of how residual MR aggravates MR, is lacking. It is therefore essential to obtain a better understanding of the biomechanical and hemodynamic influence of residual MR on the anterior leaflet post-MV repair. We developed an ex vivo left heart simulator that allowed us to quantitatively analyze valvular biomechanics and hemodynamics and elucidated the underlying clinically relevant mechanisms in mitral disease models, including models of degenerative MR,[17-21] mitral annular dilatation,[22,23] ischemic MR,[24] papillary muscle rupture,[25] Barlow's disease,[26] and rheumatic MV stenosis.[27] Throughout this series of fiber Bragg grating- (FBG) related studies, chordae linked to a prolapsed leaflet enduring a greater force than in a repaired state or at baseline, has been consistently demonstrated. Therefore, we hypothesized that excessive native primary and secondary chordal forces due to residual MR from incorrect sizing of neochordae length could result in MR progression from repetitive excessive chordal forces and eventual failure. In this study, we aimed to biomechanically evaluate the force profiles on anterior primary and secondary chordae after neochord repair for AVP with various degrees of residual MR using an ex vivo heart simulator.

METHODS

Ex Vivo Left Heart Simulator

We utilized a previously described and customized 3-dimensional (3D) modular left heart simulator to evaluate each condition of post-MV repair for AVP (Figure 1, *A*).[18,20-25] Briefly, a 3D printer (M2, Carbon 3D) was used to rapidly develop a prototype of a modular left heart coupled to a pulsatile linear actuator (ViVitro Superpump; ViVitro Labs). Pressure (Utah Medical Products Inc) and flow sensors (Carolina Medical Electronics) were incorporated to record atrial, ventricular, and aortic pressures, as well as transmitral and transaortic flow. The pulsatile pump generates a physiologic pressure waveform, whereas multiple compliance chambers regulate and attenuate pressure and flow waveforms to simulate the natural hemodynamics of the heart. A 29-mm mechanical aortic valve (St Jude Regent; Abbott Vascular) was used for the aortic position and a leakless 28-mm disc valve (ViVitro) was used as a reference valve for the mitral position to tune and calibrate the system to provide a cardiac output of approximately 5 L/minute at mean arterial pressures of 100 mm Hg, 120 mm Hg (systolic), and 80 mm Hg (diastolic). Normal saline at 37 °C was used as a test fluid to ensure appropriate conduction and operation of electromagnetic flow meters.

Sample Preparation

We obtained fresh porcine hearts (n = 8) from a meat abattoir (Animal Technologies) and dissected the MV apparatus, which included the contiguous chordae tendineae, papillary muscles, annulus, and left atrial cuff. Valves were evaluated for each experimental condition. The left atrial cuff was attached to a 3D-printed elastomeric sewing ring using a continuous polypropylene running suture. The combination of our tailored elastomeric stitching ring and the conserved cuff of left atrial tissue protected the native annulus and permitted physiologic annular mobility. Papillary muscles were fixed to carbon fiber positioning rods using interrupted 2-0 braided polyester sutures with pledgets.

Chordae Force Measurements

We previously developed precise chordae force sensors using FBG (International) technology, which operate via fiber optics.[20,22,24,26] The FBG sensor was calibrated using a precise and standardized procedure with an Instron tensile testing machine. Our FBG sensors are matched with the Instron 5848 Microtester 20 N load cell, and the strain of our sensors has been found to be less than the reported 0.1 microstrain. The accuracy and sensitivity of our calibration of the FBG sensors' measured strain conversion to forces were approximately 3% and 0.01 N, respectively, at relevant chordal forces $\leq$2 N. Each sensor was attached to a native chord by tying 2 CV-5 sutures on each side of the strain gauge. The native chord was then cut between the 2 suture attachment sites (Figure 1, *B*). The proximity to the insertion sites ensures minimal attenuation of forces due to the native elasticity of the chordae. For each valve, 2 primary and 2 secondary chordae were instrumented on both the anterior and posterior leaflets. Notably, greater pressures (particularly systolic) result in greater chordal force measurements, and because a regurgitant valve has lower hemodynamic pressures, chordal force readings are also lower. To compare force measurements accurately and consistently across repair techniques, we normalized each force measurement to the mean arterial pressure (MAP) during that specific measurement because MAP is a more accurate approximation of the average pressures, and normalization allows us to retain the most information while reducing major pressure differences. More specifically, the sensors are calibrated after implantation, while submerged, but before cardiac cycles begin. Before subjecting the valves to physiologic hemodynamics for each test condition, the sensors were recalibrated. Consequently, recorded forces measured the intracycle dynamics of chordal forces relative to the zero condition. Concerning normalization, the first step in our experiment was to gather all time-domain chordal force data with a sampling rate of approximately 1 kHz for each condition and sample, re-zeroing the data each time. Hemodynamic data was collected simultaneously for each condition and sample. For each condition and sample, 10 cycles of data were collected and the time-domain data for each cycle was averaged. To calculate the MAP for each condition and sample, the pump gain and peripheral resistances were set to generate physiologic hemodynamics and a MAP of 100 mm Hg for the baseline condition. After establishing the parameters for the baseline condition, neither the pump

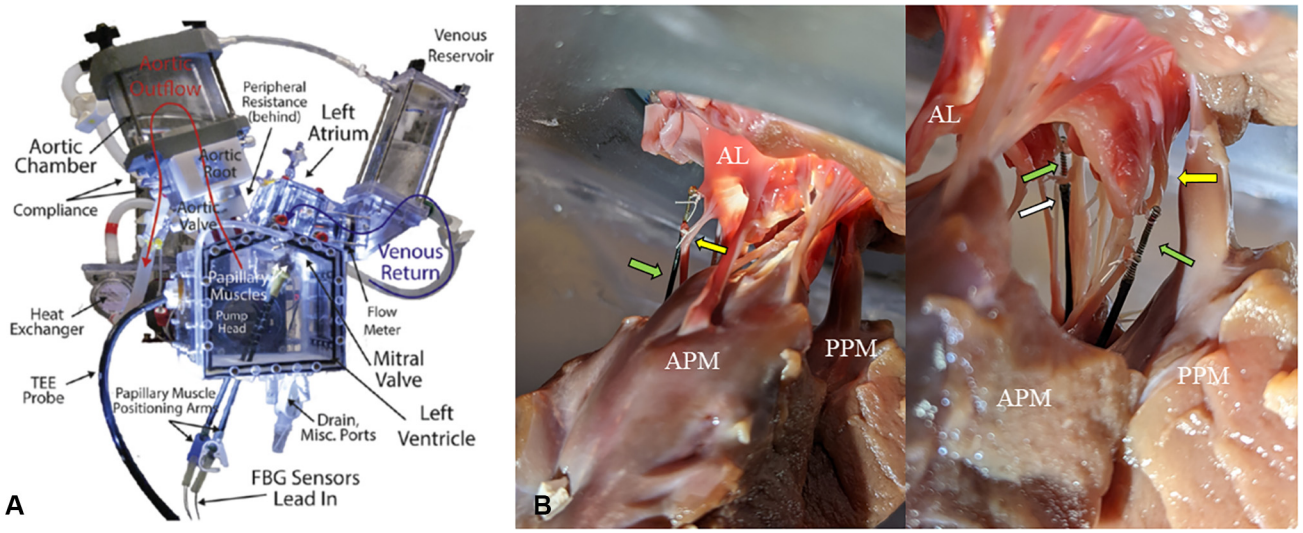

FIGURE 1. A, Schematic of Stanford *left* heart simulator in the mitral testing configuration with each component labeled. B, Close-up view of fiber Bragg gratings (*FBG*) force sensor attached to chordae tendineae of interest. *TEE*, Transesophageal echocardiogram; *AL*, anterior leaflet; *APM*, anterolateral papillary muscle; *PPM*, posteromedial papillary muscle. *Green arrows* point to FBG sensor, white arrow points to primary chordae tendineae, and *yellow arrows* point to secondary chordae tendineae.

gain nor the peripheral resistance changed with each condition for a given sample throughout the entire experiment and across all subsequent conditions. In the event of regurgitation, the pump gain was not increased to return pressures to baseline levels. To account for the decrease in forces resulting from lower pressures caused by a regurgitant condition, the entire time-series data were normalized to baseline MAP using the MAP recorded from the condition.

Study Design and Data Acquisition

Valve hemodynamics and forces were first measured at baseline. The AVP model was generated by cutting 2 primary chordae at the A2 segment and neochord repair was then performed by reinstituting the coaptation surface with 2 pairs of neochordae using CV-5 sutures anchored on both papillary muscles. To simulate post-repair residual MR, regurgitant fractions (RFs) >30% (moderate), 10% to 30% (mild), and <10% (perfect repair) were reproduced by varying neochord lengths (Figure 2 and Video 1). Hemodynamic parameters and chordal forces were analyzed after each repair. Hemodynamic data were recorded with a data acquisition system packaged with the linear pump (ViVitro Superpump; ViVitro Labs). A 1000 Hz optical interrogator (Micron Optics si255; Micron Optics) was utilized to collect FBG sensor data. Signal processing was performed with MATLAB (MathWorks). Raw measurements were averaged across 10 complete cardiac cycles. Additionally, high-speed videography (Chronos 1.4; Kron Technologies) was obtained from the en face view to qualitatively evaluate leaflet motion at 1057 frames per second.

Statistical Analysis

Continuous variables were reported as mean ± SE unless specified otherwise. To compare differences, repeated measures analysis of variance test was performed with post hoc adjustment and subsequent analysis using Tukey-Kramer test. JMP 14.0 (SAS Institute Inc) was used for statistical analysis.

RESULTS

Hemodynamic parameters are summarized in Table 1. The mitral RF of baseline, moderate, mild, and perfect repair groups were 4.7% ± 0.8%, 35.8% ± 2.1%, 19.8% ± 2.0%, and 6.0% ± 0.7%, respectively ($P < .001$). Transmitral flow and pressure tracings measured from baseline, moderate, mild, and perfect repair are illustrated in Figure 3. The regurgitant flow, marked as negative flow, during systole was substantially greater in moderate, then gradually declined in mild, before eventually returning to baseline levels for the perfect repair. Similarly, moderate was associated with decreased aortic and LV pressures compared with those measured from baseline and were gradually recovered in the mild condition. The pressure tracings normalized to baseline levels for the perfect repair condition. The peak and average values of chordal forces along with their statistical differences are detailed in Table 2. In addition, the tracings of anterior primary and secondary forces over the course of a cardiac cycle are described in Figure 4. The peak forces of the anterior primary chordae were significantly higher in the moderate condition (0.43 ± 0.06 N) compared with those of baseline (0.19 ± 0.04 N; $P = .011$), mild (0.23 ± 0.05 N; $P = .041$), and perfect repair (0.21 ± 0.03 N; $P = .006$). The average forces of the anterior primary chordae were comparable among different conditions. The average peak force of the anterior secondary chordae was significantly higher in the moderate condition (1.67 ± 0.17 N) compared with that of baseline (0.64 ± 0.13 N; $P = .003$), mild (0.84 ± 0.24 N; $P = .019$), and perfect repair (0.68 ± 0.14 N; $P = .001$). The average force of the anterior secondary chordae showed a similar trend, with moderate demonstrating a significantly higher force (0.40 ± 0.02 N) compared with that of baseline (0.17 ± 0.03 N; $P = .002$), mild (0.21 ± 0.06 N; $P = .012$), and perfect repair (0.18 ± 0.03 N; $P < .001$). No significant differences in peak and average forces on both primary and

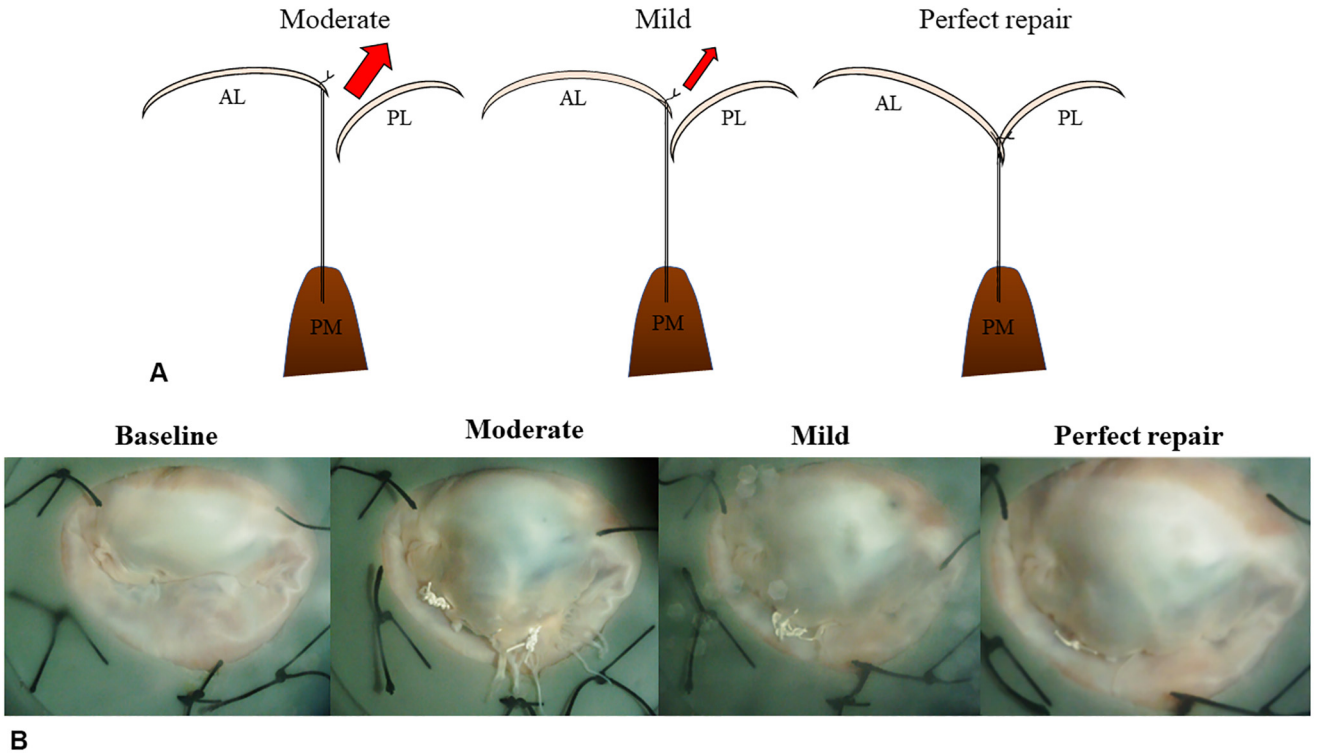

FIGURE 2. A, Scheme illustrating how to create residual mitral regurgitation (MR) after mitral valve repair. Residual MR was created by varying the neochord length. *Red arrows* showed mitral regurgitant flow. B, En face view of each valve at baseline, moderate, mild, and perfect repair after neochord repair for A2 prolapse during midsystole demonstrating leaflet. *AL*, Anterior leaflet; *PM*, papillary muscle; *PL*, posterior leaflet.

secondary anterior chordae were observed between the baseline and perfect repair conditions as well as the mild and perfect repair conditions.

DISCUSSION

In this study, we successfully created a model of postrepair residual MR by varying neochord lengths. According to our results, the peak forces on the primary and secondary chordae were significantly higher in moderate residual MR after neochord repair for AVP, compared with those of the perfect repair. In a normal valve, the systolic stresses are distributed among the primary and secondary chordae, which are differentiated by their relative thicknesses and positions on the leaflet. In cases of a properly coapting valve with mild to no MR, during systole, the valve is supported by the chordae, which function primarily to position the leaflets because a large proportion of the stresses are distributed between the leaflets into the coaptation plane. This translates to a relatively low level of tensile loading and stresses distributed directly to the chordae.[28] However, upon prolapse and significant regurgitant flow, these chordae are exposed to a much larger proportion of the systolic pressures that have been translated to tensile forces on the leaflet. These forces should have been distributed across the coaptated anterior leaflet surface and relevant supporting chordae tendineae. These increased forces are due to a combination of decreased coaptation, which has been shown to increase the valvular surface area and subsequent forces of the leaflets exposed to the transmitral pressure gradient,[29] and an increase in dynamic form drag from the regurgitant flow. These increased stresses, in turn, can cause further deterioration, remodeling, and even failure of the remaining chordae as fatigue damage amplifies via the long-term cyclic loading of the valvular system. In short, the prolapsed anterior leaflet in moderate MR was exposed to

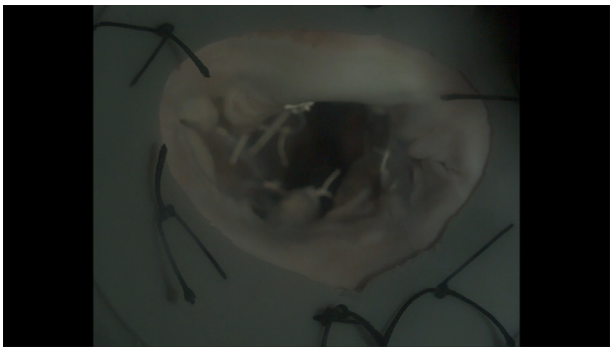

VIDEO 1. En face view of high-speed videometric footage highlighting baseline, moderate, mild, and perfect repair postneochord repair for A2 prolapse. Video available at: https://www.jtcvs.org/article/S2666-2736(23)00101-8/fulltext.

TABLE 1. Hemodynamic parameters in the conditions of baseline, moderate, mild, and perfect repair

Variable	Baseline	Moderate	Mild	Perfect repair	*P* value
Aortic systolic pressure (mm Hg)	123.5 ± 1.7	82.8 ± 4.6	105.3 ± 7.3	127.1 ± 3.2	<.001
Aortic diastolic pressure (mm Hg)	87.1 ± 2.0	58.0 ± 3.9	75.7 ± 6.0	91.4 ± 2.6	<.001
Arterial mean pressure (mm Hg)	102.3 ± 1.5	69.0 ± 4.3	88.2 ± 6.4	106.2 ± 2.6	<.001
Atrial mean pressure (mm Hg)	7.2 ± 0.8	11.8 ± 1.1	9.4 ± 1.1	8.7 ± 1.1	.100
Ventricular mean pressure (mm Hg)	43.5 ± 1.1	28.4 ± 1.7	36.0 ± 2.5	44.7 ± 1.3	<.001
Heart rate (bpm)	70 ± 0	70 ± 0	70 ± 0	70 ± 0	.901
Pump stroke volume (mL)	110.0 ± 0.0	110.0 ± 0.0	110.0 ± 0.0	110.1 ± 0.0	.168
Cardiac output (L/min)	3.5 ± 0.5	4.5 ± 0.5	3.9 ± 0.5	3.4 ± 0.5	.346
Mitral regurgitant fraction (%)	4.7 ± 0.8	35.8 ± 2.1	19.8 ± 2.0	6.0 ± 0.7	<.001
Mitral forward volume (mL)	50.0 ± 7.5	64.7 ± 6.9	55.2 ± 7.3	48.9 ± 6.5	.347
Mitral closing volume (mL)	6.2 ± 0.7	13.5 ± 2.8	9.2 ± 1.1	7.4 ± 1.0	.028
Mitral leakage volume (mL)	2.2 ± 0.3	22.7 ± 2.2	10.4 ± 1.3	2.7 ± 0.4	<.001
Transmitral mean pressure (mm Hg)	102.6 ± 4.4	66.5 ± 5.2	89.3 ± 8.1	108.4 ± 3.6	<.001

Values are presented as mean ± SE.

a substantially greater fraction of the systolic regurgitant pressures, resulting in greater tensile stresses on the leaflet. These enhanced forces were the result of diminished coaptation and an increase in dynamic form drag from regurgitant flow, resulting in a greater force on chordae attached to the prolapsed anterior leaflet, although LV dilation due to persistent MR and subsequent valve tethering would be among the mechanisms of progressive MR particularly in the late phase. It would be easier to comprehend if we analyzed forces on neochords for which the outcomes should be more evident, but this scope needs further assessment and will be evaluated in subsequent studies. Our biomechanical knowledge supports the fact that moderate residual postrepair MR exaggerates the influence of systolic stresses on the native chordae, which could progress to severe MR necessitating reoperation.[8,9]

Additionally, our results indicate that moderate residual MR was associated with significantly higher stresses on both primary and secondary chordae compared with mild residual MR. Based on the mechanical point of view described above, the extent of coaptation length, which typically decreases as the MR grade progresses, would influence the stresses on secondary chordae as well as primary chordae at the peak of systole.[29] Further, patients with

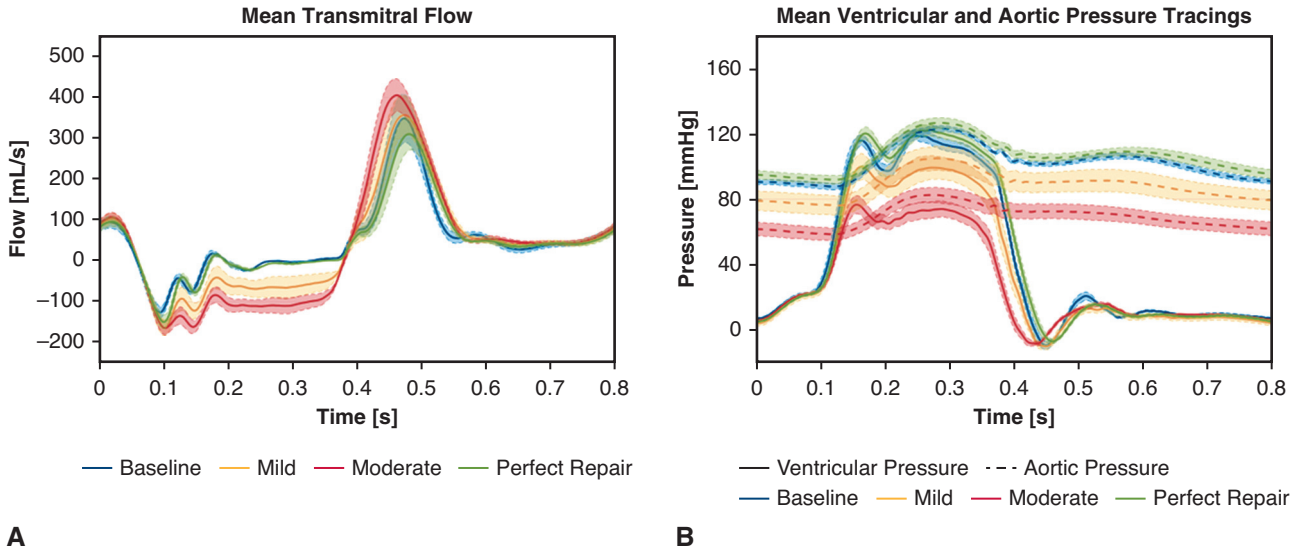

FIGURE 3. Transmitral flow (A) and pressure tracings (B) measured from baseline, moderate, mild, and perfect repair. Note that the flow reversal during systole was substantially greater and the aortic and *left* ventricular pressures were substantially lower in moderate, compared with perfect repair as well as baseline. *Shaded areas* represent SE.

TABLE 2. The peak and average forces of interest

	Group	Mean ± SE	ANOVA	*P* value for difference			
				Baseline	Moderate	Mild	Perfect repair
AP peak force (N)	Baseline	0.19 ± 0.04	.004*	Reference	.011*	.946	.996
	Moderate	0.43 ± 0.06		.011*	Reference	.041*	.006*
	Mild	0.23 ± 0.05		.946	.041*	Reference	.980
	Perfect repair	0.21 ± 0.03		.996	.006*	.980	Reference
AP averaged force (N)	Baseline	0.05 ± 0.01	.233	Reference	.518	.980	.995
	Moderate	0.07 ± 0.01		.518	Reference	.297	.276
	Mild	0.04 ± 0.01		.980	.297	Reference	.998
	Perfect repair	0.04 ± 0.01		.995	.276	.998	Reference
AS peak force (N)	Baseline	0.64 ± 0.13	<.001*	Reference	.003*	.871	.998
	Moderate	1.67 ± 0.17		.003*	Reference	.019*	.001*
	Mild	0.84 ± 0.24		.871	.019*	Reference	.902
	Perfect repair	0.68 ± 0.14		.998	.001*	.902	Reference
AS average force (N)	Baseline	0.17 ± 0.03	<.001*	Reference	.002*	.883	.998
	Moderate	0.40 ± 0.02		.002*	Reference	.012*	<.001*
	Mild	0.21 ± 0.06		.883	.012*	Reference	.917
	Perfect repair	0.18 ± 0.03		.998	<.001*	.917	Reference

Values are presented as mean ± SE. *SE*, Standard error; *ANOVA*, analysis of variance; *AP*, anterior primary; *N*, Newton; *AS*, anterior secondary. *Statistically significant $P < .05$.

moderate residual MR often progress to severe MR shortly after surgery. Although the majority of mild cases remain mild, some of them progress slowly and develop severe MR immediately after they become moderate.[3,9] This finding can be explained by the theory that procedure-related failure, such as incomplete repair due to

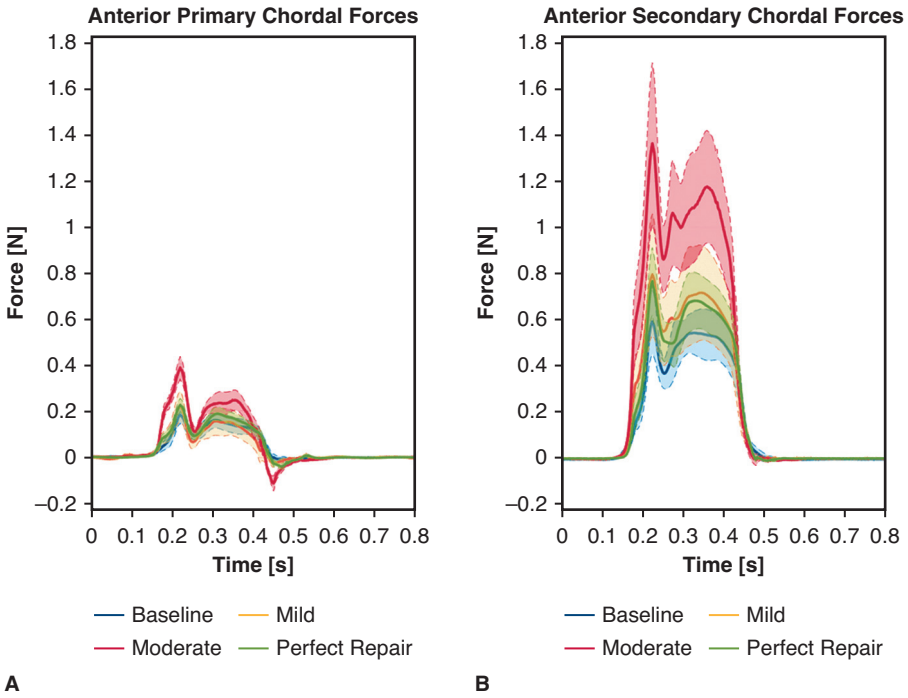

FIGURE 4. Averaged chordal force tracings over the course of a cardiac cycle from anterior primary (A) and secondary chordae (B) in the anterior valve prolapse model after neochord repair. Note that the peak forces of the anterior primary and secondary chordae were significantly higher in the moderate condition compared with those of baseline, mild, and perfect repair conditions. Shaded areas represent SE.

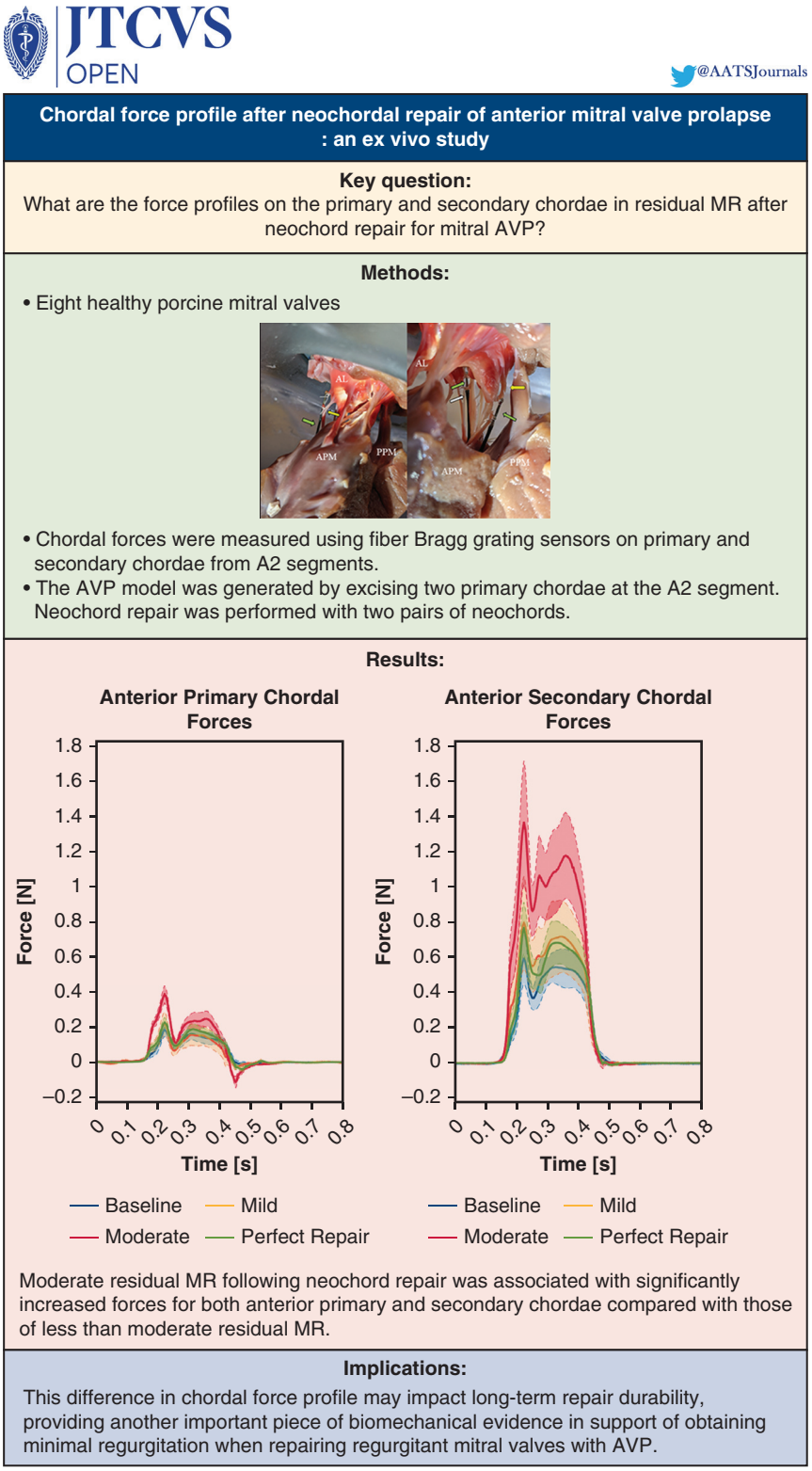

FIGURE 5. Chordal force profile after neochordal repair of anterior mitral valve prolapse: An ex vivo study. *MR*, Mitral regurgitation; *AVP*, anterior mitral valve prolapse; *AL*, anterior leaflet; *APM*, anterolateral papillary muscle; *PPM*, posteromedial papillary muscle.

inappropriate neochord length estimation, is associated with rapid deterioration in the short term after MV repair, whereas valve-related failure, such as progressive degenerative disease, is related to slow, steady decline over the long term.[30] A possible factor exacerbating neochord length inaccuracy during MV repair surgery is that neochord length is assessed upon static LV pressurization, leading to a repair inspection while the LV is dilated in its physiologically contracted state. Thus, competence testing may lead to an overestimation in neochord length constituting a mechanically deficient repair.[31] Therefore, moderate residual MR should be considered a failure of the procedure, whereas mild residual MR should be considered a failure associated with the valve. According to a report by Kim and colleagues,[9] patients with mild residual MR at discharge deteriorated relatively slowly, with 50% of patients progressing to moderate or greater MR over 5 years after repair. However, patients with moderate or greater residual MR at discharge worsened rapidly within a few years, resulting in approximately 80% of patients deteriorating at 5 years postoperation.[9] Our biomechanical results help to explain these clinical outcomes by identifying the significant differences in chordal stresses between moderate and mild residual MR.

Some investigations have revealed that even mild residual MR after repair increases the chance of eventual repair failure necessitating reoperation.[3,5,9,15] However, no difference was found in the peak and average forces on the primary and secondary chordae between mild and perfect repair in our study. As described above, if there is some coaptation, secondary chordae are able to share the stress with primary chordae, minimizing the stress on both chords. When the moderately prolapsed leaflet has been exposed to minor regurgitant stress for an extended period, gradual valve degeneration and substantial MR might develop.

This study has several limitations. One limitation is that a non-significant difference would not directly reflect the long-term results because the current results were acquired with a restricted duration of 10 cardiac cycles; however, a significant difference should have a great influence on the long-term outcomes as well as the short-term outcomes. Another limitation is that RF utilized for the current study was obtained from mechanically analyzed flow data in our ex vivo left heart simulator, not from the echocardiographic analysis. Clinical MR grade is determined by using the measurements obtained from Doppler echocardiography[32,33]; therefore, our MR criteria would not perfectly match the clinical criteria. However, we believe that the current RF is a real calculated value as accurate as the clinically utilized RF. Our next step will be to evaluate MR with echocardiography and long-term follow-up in a large-scale animal model study to explore these repairs in vivo and thus overcome these limitations. Furthermore, our disease model predominantly replicated the acute MR pathology, whereas the vast majority of clinically observed MV prolapses are chronic and characterized by a dilated mitral annulus. Hence, our ex vivo model was incapable of simulating the chronic adaptation and alterations that occur in the MV apparatus. In vivo tests on chronic MR models of large animals may be warranted to further validate our study's findings. Each valve has its unique anatomy and chordal distributions and lengths; therefore, it was difficult to standardize neochordae lengths to achieve clinically relevant RF. For this study, we aimed to adjust the neochord length until our desired target RF was achieved. Different neochordal lengths may result in a degree of force variation for each condition. Regarding normalization, whereas we chose to normalize chordal force measurements to MAP, transmitral gradient would be a more accurate pressure condition to use. Functionally, normalizing to either MAP or transmitral pressure gradient metrics yields very similar results, with identical values and statistical outcomes (data not shown). Therefore, our normalization to MAP is sufficient, but the more accurate transmitral pressure gradient could also be used for normalization. Lastly, the inability to employ human mitral valves forced us to use porcine valves instead. However, the geometry of the leaflets, annulus, and papillary muscles, as well as the density and cellular composition of the chordae tendineae, are quite comparable in porcine valves.[34,35]

CONCLUSIONS

In our ex vivo AVP model, moderate residual MR following neochord repair was significantly associated with increased forces for both anterior primary and secondary chordae compared with those of less-than-moderate residual MR (Figure 5). This difference in chordal force profile may influence long-term repair durability, providing another important piece of biomechanical evidence in support of obtaining minimal regurgitation when repairing regurgitant mitral valves with AVP.

Conflict of Interest Statement

The authors reported no conflicts of interest.

The *Journal* policy requires editors and reviewers to disclose conflicts of interest and to decline handling or reviewing manuscripts for which they may have a conflict of interest. The editors and reviewers of this article have no conflicts of interest.

The authors thank Mr Kevin Taweel and the Rittenberg Family Foundation for the generous donation to support this research effort and Taichi Sakaguchi for giving us a hint of the study concept and educational insights into our research.

References

1. Bowdish ME, D'Agostino RS, Thourani VH, Schwann TA, Krohn C, Desai N, et al. STS Adult Cardiac Surgery Database: 2021 update on outcomes, quality, and research. *Ann Thorac Surg*. 2021;111:1770-80.

2. De Bonis M, Lapenna E, Lorusso R, Buzzatti N, Gelsomino S, Taramasso, et al. Very long-term results (up to 17 years) with the double-orifice mitral valve repair combined with ring annuloplasty for degenerative mitral regurgitation. *J Thorac Cardiovasc Surg*. 2012;144:1019-24.
3. Suri RM, Clavel MA, Schaff HV, Michelena HI, Huebner M, Nishimura RA, et al. Effect of recurrent mitral regurgitation following degenerative mitral valve repair: long-term analysis of competing outcomes. *J Am Coll Cardiol*. 2016;67:488-98.
4. De Bonis M, Lapenna E, Taramasso M, Canna GL, Buzzatti N, Pappalardo F, et al. Very long-term durability of the edge-to-edge repair for isolated anterior mitral leaflet prolapse: up to 21 years of clinical and echocardiographic results. *J Thorac Cardiovasc Surg*. 2014;148:2027-32.
5. Tabata M, Kasegawa H, Fukui T, Shimizu A, Sato Y, Takanashi S. Long-term outcomes of artificial chordal replacement with tourniquet technique in mitral valve repair: a single-center experience of 700 cases. *J Thorac Cardiovasc Surg*. 2014;148:2033-8.
6. Hata H, Fujita T, Shimahara Y, Sato S, Ishibashi-Ueda H, Kobayashi J. A 25-year study of chordal replacement with expanded polytetrafluoroethylene in mitral valve repair. *Interact Cardiovasc Thorac Surg*. 2015;20:463-8; discussion 468.
7. David TE, Armstrong S, McCrindle BW, Manlhiot C. Late outcomes of mitral valve repair for mitral regurgitation due to degenerative disease. *Circulation*. 2013;127:1485-92.
8. Murashita T, Okada Y, Fujiwara H, Kanemitsu H, Fukunaga N, Konishi Y, et al. Mechanism of and risk factors for reoperation after mitral valve repair for degenerative mitral regurgitation. *Circ J*. 2013;77:2050-5.
9. Kim JH, Lee SH, Joo HC, Youn YN, Yoo KJ, Chang BC, et al. Effect of recurrent mitral regurgitation after mitral valve repair in patients with degenerative mitral regurgitation. *Circ J*. 2017;82:93-101.
10. Sugiura A, Kavsur R, Spieker M, Iliadis C, Goto T, Ozturk C, et al. Recurrent mitral regurgitation after MitraClip: predictive factors, morphology, and clinical implication. *Circ Cardiovasc Interv*. 2022;15:e010895.
11. Kar S, Mack MJ, Lindenfeld J, Abraham WT, Asch FM, Weissman NJ, et al. Relationship between residual mitral regurgitation and clinical and quality-of-life outcomes after transcatheter and medical treatments in heart failure: COAPT Trial. *Circulation*. 2021;144:426-37.
12. Kar S, Feldman T, Qasim A, Trento A, Kapadia S, Pedersen W, et al. Five-year outcomes of transcatheter reduction of significant mitral regurgitation in high-surgical-risk patients. *Heart*. 2019;105:1622-8.
13. Ailawadi G, Lim DS, Mack MJ, Trento A, Kar S, Grayburn PA, et al. One-year outcomes after MitraClip for functional mitral regurgitation. *Circulation*. 2019;139:37-47.
14. Sato H, Cavalcante JL, Bae R, Enriquez-Sarano M, Bapat VN, Gossl M, et al. Hemodynamic profiles and clinical response to transcatheter mitral repair. *JACC Cardiovasc Interv*. 2022;15:1697-707.
15. Morisaki A, Takahashi Y, Fujii H, Sakon Y, Murakami T, Shibata T. Outcomes of loop technique with ring annuloplasty: a >10-year experience. *Gen Thorac Cardiovasc Surg*. 2022;70:793-803.
16. David TE, Armstrong S, Ivanov J. Chordal replacement with polytetrafluoroethylene sutures for mitral valve repair: a 25-year experience. *J Thorac Cardiovasc Surg*. 2013;145:1563-9.
17. Pandya PK, Wilkerson RJ, Imbrie-Moore AM, Zhu Y, Marin-Cuartas M, Park MH, et al. Quantitative biomechanical optimization of neochordal implantation location on mitral leaflets during valve repair. *J Thorac Cardiovasc Surg Tech*. 2022;14:89-93.
18. Paulsen MJ, Cuartas MM, Imbrie-Moore A, Wang H, Wilkerson R, Farry J, et al. Biomechanical engineering comparison of four leaflet repair techniques for mitral regurgitation using a novel 3-dimensional-printed left heart simulator. *J Thorac Cardiovasc Surg Tech*. 2021;10:244-51.
19. Marin-Cuartas M, Imbrie-Moore AM, Zhu Y, Park MH, Wilkerson R, Leipzig M, et al. Biomechanical engineering analysis of commonly utilized mitral neochordae. *J Thorac Cardiovasc Surg Open*. 2021;8:263-75.
20. Paulsen MJ, Imbrie-Moore AM, Wang H, Bae JH, Hironaka CE, Farry JM, et al. Mitral chordae tendineae force profile characterization using a posterior ventricular anchoring neochordal repair model for mitral regurgitation in a three-dimensional-printed ex vivo left heart simulator. *Eur J Cardio Thorac Surg*. 2020;57:535-44.
21. Imbrie-Moore AM, Paulsen MJ, Thakore AD, Wang H, Hironaka CE, Lucian HL, et al. Ex vivo biomechanical study of apical versus papillary neochord anchoring for mitral regurgitation. *Ann Thorac Surg*. 2019;108:90-7.
22. Zhu Y, Imbrie-Moore AM, Wilkerson RJ, Paulsen MJ, Park MH, Woo YJ. Ex vivo biomechanical analysis of flexible versus rigid annuloplasty rings in mitral valves using a novel annular dilation system. *BMC Cardiovasc Disord*. 2022;22:73.
23. Imbrie-Moore AM, Paullin CC, Paulsen MJ, Grady F, Wang H, Hironaka CE, et al. A novel 3D-printed preferential posterior mitral annular dilation device delineates regurgitation onset threshold in an ex vivo heart simulator. *Med Eng Phys*. 2020;77:10-8.
24. Imbrie-Moore AM, Zhu Y, Bandy-Vizcaino T, Park MH, Wilkerson RJ, Woo YJ. Ex vivo model of ischemic mitral regurgitation and analysis of adjunctive papillary muscle repair. *Ann Biomed Eng*. 2021;49:3412-24.
25. Marin-Cuartas M, Zhu Y, Imbrie-Moore AM, Park MH, Wilkerson RJ, Leipzig M, et al. Biomechanical engineering analysis of an acute papillary muscle rupture disease model using an innovative 3D-printed left heart simulator. *Interact Cardiovasc Thorac Surg*. 2022;34:822-30.
26. Imbrie-Moore AM, Paulsen MJ, Zhu Y, Wang H, Lucian HJ, Farry JM, et al. A novel cross-species model of Barlow's disease to biomechanically analyze repair techniques in an ex vivo left heart simulator. *J Thorac Cardiovasc Surg*. 2021;161:1776-83.
27. Park MH, Pandya PK, Zhu Y, Mullis DM, Wang H, Imbrie-Moore AM, et al. A novel rheumatic mitral valve disease model with ex vivo hemodynamic and biomechanical validation. *Cardiovasc Eng Technol*. 2023;14:129-40.
28. Nazari S, Carli F, Salvi S, Banfi C, Aluffi A, Mourad Z, et al. Patterns of systolic stress distribution on mitral valve anterior leaflet chordal apparatus. A structural mechanical theoretical analysis. *J Cardiovasc Surg*. 2000;41:193-202.
29. Park MH, van Kampen A, Melnitchouk S, Wilkerson RJ, Nagata Y, Zhu Y, et al. Native and post-repair residual mitral valve prolapse increases forces exerted on the papillary muscles: a possible mechanism for localized fibrosis? *Circ Cardiovasc Interv*. 2022;15:e011928.
30. Dumont E, Gillinov AM, Blackstone EH, Sabik JF III, Svensson LG, Mihaljevic T, et al. Reoperation after mitral valve repair for degenerative disease. *Ann Thorac Surg*. 2007;84:444-50; discussion 450.
31. Park MH, Marin-Cuartas M, Imbrie-Moore AM, Wilkerson RJ, Pandya PK, Zhu Y, et al. Biomechanical analysis of neochordal repair error from diastolic phase inversion of static left ventricular pressurization. *J Thorac Cardiovasc Surg Tech*. 2022;12:54-64.
32. Otto CM, Nishimura RA, Bonow RO, Carabello BA, Erwin JP III, Gentile F, et al. 2020 ACC/AHA guideline for the management of patients with valvular heart disease: a report of the American College of Cardiology/American Heart Association Joint Committee on Clinical Practice Guidelines. *J Thorac Cardiovasc Surg*. 2021;162:e183-353.
33. Zoghbi WA, Adams D, Bonow RO, Enrique-Sarano M, Foster E, Grayburn PA, et al. Recommendations for noninvasive evaluation of native valvular regurgitation: a report from the American Society of Echocardiography developed in collaboration with the Society for Cardiovascular Magnetic Resonance. *J Am Soc Echocardiogr*. 2017;30:303-71.
34. Millington-Sanders C, Meir A, Lawrence L, Stolinski C. Structure of chordae tendineae in the left ventricle of the human heart. *J Anat*. 1998;192:573-81.
35. Crick SJ, Sheppard MN, Ho SY, Gebstein L, Anderson RH. Anatomy of the pig heart: comparisons with normal human cardiac structure. *J Anat*. 1998;193:105-19.

Key Words: mitral valve, mitral valve prolapse, anterior valve prolapse, mitral valve repair, neochord repair, residual mitral regurgitation, force profile